Supporting information

Supplemental figure legends

Fig. S1. Phenotypes of Adipo-*Zip13*KO mice associated with beige adipocyte biogenesis

(A, B) Whole-body oxygen consumption of 23-week-old Ctrl (n = 8) and Adipo-*Zip13*KO (n = 9) mice fed a STD. (A): VO_2 trend, (B): VO_2 period. (C) Food intake of 21- to 24-week-old Ctrl (n = 6) and Adipo-*Zip13*KO (n = 7) mice fed a STD. (D) Locomotor activity of 23-week-old Ctrl (n = 8) and Adipo-*Zip13*KO (n = 9) mice fed a STD. (E) Rectal temperatures of 21- to 24-week-old Ctrl (n = 6) and Adipo-*Zip13*KO (n = 7) mice fed a STD. (F) Relative mRNA expression of the indicated genes in the subcutaneous fat tissue of 34-week-old Ctrl (n = 6) and Adipo-*Zip13*KO (n = 6) mice fed a STD. (G) Hematoxylin and eosin (H&E) staining of subcutaneous fat and brown fat tissues from Ctrl and Adipo-*Zip13*KO mice (left). Scale bars = 100 μm. Quantification results of adipocytes sizes measured from the H&E-stained sections of subcutaneous fat and brown fat tissues of Ctrl (n = 3) and Adipo-*Zip13*KO (n = 3) mice (right). (H) Whole-body oxygen consumption (VO_2) of 24-week-old Ctrl (n = 9) and Adipo-*Zip13*KO (n = 7) mice fed a STD at the indicated temperature. (I) Relative mRNA expression of the indicated genes from the subcutaneous fat tissue of the mice analyzed in (H). Ctrl (n = 9), Adipo-*Zip13*KO mice (n = 7). Data are shown as the mean ± SEM. In (B, C, D, E, F, and I), $^{*}p < 0.05$, and $^{****}p < 0.0001$, by the two-tailed unpaired Student *t*-test. In (G), data were analyzed by multiple two-tailed unpaired *t*-tests. Circles indicate the data of individual mice. ns, not significant.

Fig. S2. Adipo-*Zip13*KO mice have reduced RER

(A) (A, B) Whole-body RER of 33-week-old Ctrl (n = 8) and Adipo-*Zip13*KO (n = 9) mice fed a STD.

(A): RER trend, (B): RER period. (C) Plasma NEFA levels of 12- to 16-week-old Ctrl (n = 8) and Adipo-*Zip13*KO female mice (n = 13) fasted overnight and intraperitoneal (i.p.) injected with the β3-adrenergic receptor agonist CL316,243. (D) NEFA release from the indicated fat explants treated with saline (Basal) or isoproterenol (Iso). Fold changes are shown as stimulated/basal lipolysis. Analyzed fat pads were from 28- to 32-week-old Ctrl (n = 6) and Adipo-*Zip13*KO mice (n = 7). (E) The expression of *Zip13* and adipocyte differentiation markers in Ctrl (n = 3) and Adipo-*Zip13*KO (n = 3) mature adipocyte cells. (F) Relative mRNA expression of the indicated genes in 34-week-old Ctrl (n = 5) and Adipo-*Zip13*KO (n = 4) mice on a STD. Data are shown as the mean ± SEM. In (B, D, E, and F), $*p < 0.05$ and $**p < 0.01$, by the two-tailed unpaired Student *t*-test. In (C), $*p < 0.05$ and $****p < 0.0001$, by two-way ANOVA followed by Dunnett's multiple comparisons test. Circles indicate the data of individual mice.

Fig. S3. Adipo-*Zip13*KO mice showed resistance to the development of insulin resistance

(A) Lean mass (left) and fat mass (right) of 32 to 33-week-old Ctrl (n = 8) and Adipo-*Zip13*KO mice (n = 9) fed a STD. (B) Micro-computed tomography (CT) evaluation of visceral fat mass and subcutaneous fat mass of 32 to 33-week-old Ctrl (n = 8) and Adipo-*Zip13*KO mice (n = 9) fed a STD. (C) Blood glucose concentrations were measured during intraperitoneal glucose tolerance test (IPGTT) in 31 to 32-week-old Ctrl (n = 6) and Adipo-*Zip13*KO (n = 9) mice fed a STD. (D) Insulin concentrations related to of the mice analyzed in (C). (E) Insulin tolerance testing of 19-week-old Ctrl (n = 8) and Adipo-*Zip13*KO (n = 14) mice fed a HFD for 13 weeks. (F) Rectal body temperatures during acute cold exposure (4 °C) in fasted 55-week-old Ctrl (n = 9) and Adipo-*Zip13*KO mice (n = 6). (G) Oxygen consumption rates of 21- to 25-week-old Ctrl (n = 12) and Adipo-*Zip13*KO (n = 13)

female mice injected with CL316,243 (0.5 mg/kg) under thermoneutral conditions. Data are shown as the mean ± SEM. In (A, B, C, D, E, and F), $^{*}p < 0.05$ and $^{**}p < 0.01$, by the two-tailed unpaired Student *t*-test. In (G), $^{*}p < 0.05$ and $^{****}p < 0.0001$, by two-way ANOVA followed by the Tukey's multiple comparison test. Circles indicate the data of individual mice.

Fig. S4. Accelerated cAMP/PKA signaling pathway in white fat tissue of Adipo-*Zip13*KO mice

(A) FerroOrange and ER tracker staining in mature adipocytes. Scale bar: 50 μm (left panel), 10 μm (right panel). (B) Hydroxyl radical levels in Ctrl (n = 5) and Adipo-*Zip13*KO (n = 5) mature adipocytes. (C) Immunoblotting of pPKA, PKA, pHSL, HSL, pCREB, CREB, and GAPDH in Ctrl and Adipo-*Zip13*KO mature adipocyte cells stimulated with DMSO (Basal) or isoproterenol (Iso) (top). Quantification of pPKA, pHSL, and pCREB proteins normalized to PKA, HSL, and CREB, respectively (bottom). In (B), $^{**}p < 0.01$ and $^{****}p < 0.0001$, by two-way ANOVA followed by the Tukey's multiple comparison test. In (C), $^{*}p < 0.05$, $^{**}p < 0.01$, and $^{****}p < 0.0001$, by the two-tailed unpaired Student *t*-test. Circles indicate the data of individual samples.

Fig. S5. PDE3 activity is reduced in Adipo-*Zip13*KO cells

(A) NEFA release from the differentiated Ctrl (n = 4) and Adipo-*Zip13*KO cells (n = 4), stimulated with cilostamide (PDE3 inhibitor), or rolipram (PDE4 inhibitor). (B) NEFA release from mature adipocytes isolated from subcutaneous adipose tissues of Ctrl and Adipo-*Zip13*KO mice in the presence of the PDE3 inhibitor cilostamide and the PDE4 inhibitor rolipram under isoproterenol (Iso) stimulation. Mature adipocytes were obtained from 23- to 36-week-old Ctrl (n = 12) and Adipo-*Zip13*KO mice (n = 12). NEFA release into the medium was normalized to the basal control group.

(C) Relative expression of *Pde3b* in the indicated cells. (D) Released NEFA levels of Ctrl and Adipo-*Zip13*KO cells transfected with scrambled siRNA or siRNA against *Pde3b* under the isoproterenol stimulation. Data are shown as the mean ± SEM. In (A), $^{**}p < 0.01$, by two-way ANOVA followed by the Bonferroni's multiple comparison test. ns, not significant. In (B), $^{*}p < 0.05$ by two-way ANOVA followed by the Tukey's multiple comparisons test. In (C), $^{****}p < 0.0001$ by two-way ANOVA followed by the Tukey's multiple comparison test. In (D), $^{*}p < 0.05$, $^{**}p < 0.01$, data were analyzed by the two-tailed unpaired Student *t*-test.

Fig. S6. Accelerated cAMP/PKA signaling pathway in brown fat tissue of Adipo-*Zip13*KO mice

(A) Immunoblotting of pPKA, PKA, pCREB, CREB, Ucp1 and GAPDH in brown fat tissues from 22 to 44-week-old Ctrl and Adipo-*Zip13*KO mice after treatment with isoproterenol (Iso) (n = 7 mice each) (top panels). Phosphorylation levels in the upper panels were normalized by total protein (low bar graphs). (B) Fe^{2+} level in Ctrl and Adipo-*Zip13*KO mature adipocyte cells. Fe^{2+} level was detected using FerroOrange. (C) Immunoblotting of IRP2, TfR, FTL, Fth1, aP2, and actin using whole cell extracts of differentiated Ctrl and Adipo-*Zip13*KO cells treated with isoproterenol (Iso) Actin was included as a loading control. Each protein was quantified by normalization to actin. Data are shown as the mean ± SEM. $^{*}p < 0.05$, $^{**}p < 0.01$, and $^{***}p < 0.001$, data were analyzed by the two-tailed unpaired Student *t*-test.

Fig. S7. Membrane topology of 4F2hc-m13-HA

Immunofluorescence staining of mZIP13-HA and 4F2hc-m13-HA using an anti-HA antibody in live *X. laevis* oocytes. The white arrowhead indicates the HA signal. DIC: differential interference contrast

image; Scale bars: 50 μm

Fig. S8. Zn^{2+} and Fe^{2+} transport kinetics of 4F2hc-m13

(A) Time course of zinc uptake by 4F2hc-m13. Zn^{2+} uptake (100 μM) increased linearly for up to 240 min. wi, water injection. (B) Michaelis-Menten fit of the concentration-dependent uptake of Zn^{2+}. The calculated Km is 130 μM, and the V_{max} is 158 fmol/oocyte/min. Zn^{2+} uptake was observed for 120 min. Inset, Eadie-Hofstee plot. (C) Time course of Fe^{2+} uptake (100 μM) by 4F2hc-m13. (D) Michaelis-Menten fit of the concentration-dependent uptake of Fe^{2+}. The calculated Km is 137 μM, and the V_{max} is 78 fmol/oocyte/min. Fe^{2+} uptake was observed for 120 min. All data are shown as the mean ± SEM (n = 5-9 for the time course assays, n = 14-22 for the Zn^{2+} concentration-dependence assay, and n = 21-34 for the Fe^{2+} concentration-dependence assay). V, velocity; V/S, velocity per metal concentration.

Fig. S9. The expression of ZIP13-WT and ZIP13-H254A in preadipocyte and mature adipocyte

(A) The protein expression of ZIP13-HA at day 0 and 6 of differentiation induction in Adipo-*Zip13*KO preadipocytes expressing ZIP13(WT) and ZIP13(H254A). (B) NEFA release from Adipo-*Zip13*KO mature adipocyte cells expressing ZIP13-WT or ZIP13-H254A, and treated with DMSO (Basal) and isoproterenol (Iso). (C) The expression of adipocyte differentiation markers in Adipo-*Zip13*KO mature adipocyte cells expressing ZIP13(WT) and ZIP13(H254A). Data are shown as the mean ± SEM. In (B), $^{****}p < 0.0001$, by two-way ANOVA followed by the Tukey' multiple comparison test. In (C), $^{**}p < 0.01$, $^{***}p < 0.001$, and $^{****}p < 0.0001$, by one-way ANOVA followed by the Tukey's multiple comparison test. Circles indicate the data of individual samples. ns, not significant.

Fig. S10. Zinc and iron levels in subcutaneous and visceral adipose tissues of Ctrl mice

Fe and Zn contents (left and middle panels, respectively), and Fe/Zn ratios (right panel) in subcutaneous and visceral adipose tissues of Ctrl mice. Data are shown as the mean ± SEM; $^{*}p < 0.05$ and $^{**}p < 0.01$, by the two-tailed unpaired Student *t*-test. Circles indicate the data of individual mice.

Fig. S11. Mitochondrial Fe^{2+} levels are decreased in Adipo-*Zip13*KO mature adipocyte cells

Single-cell signal intensities of Mito-FeroGreen normalized by area. $^{****}p < 0.0001$, by the two-tailed unpaired Student *t*-test.

Fig. S12. Strategy of the conditional KO at the *Zip13* locus

The black boxes indicate exons of the *Zip13* gene. Pr DT-A pA is the diphtheria toxin A fragment gene directed by the MC1 promoter for negative selection. Pr Puro pA and Pr Neo pA driven by the PGK1 promoter are the drug-resistance genes for positive selection in ES cells. The cassettes flanked by F3 or FRT sequences are excised by flippase to generate the Flox allele. The KO allele is generated using a tissue-specific Cre mouse. P1, P2, P3, and P4 are primers for genotyping PCR.

Fig. S13. VO_2 and RER in *Zip13$^{f/f}$-Adiponectin-Cre* mice

(A) Whole-body oxygen consumption of 19-week-old *Zip13$^{f/f}$* (n = 10) and *Zip13$^{f/f}$-Adiponectin-Cre* mice (n = 13) fed a STD. (B) Whole-body RER of 19-week-old *Zip13$^{f/f}$* (n = 10) and *Zip13$^{f/f}$-Adiponectin-Cre* mice (n = 13) fed a STD. (C) Relative expression level in brown adipose tissue and subcutaneous adipose tissue from mice of each genotype at 14 to 22 weeks of age (n = 2–6). Data are

shown as the mean ± SEM. Circles indicate the data of individual mice.

Fig. S14. Superimposition of mZIP13 and 4F2hc-m13 (five models)

The predicted models of 4F2hc-m13 were superimposed onto the transmembrane region of the structural model of mouse ZIP13 (PDB ID: Q8BZH0) deposited in AlphaFold DB, and the root-mean-square deviation of atomic positions (RMSD) values were calculated using Mol* Viewer.

Fig. S15. Superimposition of 4F2hc-m13 (rank 1) to the other rank models

The top-ranked predicted model of 4F2hc-m13 (rank 1) was superimposed onto the transmembrane regions of the m13 domains of the other models. The RMSD values were calculated using Mol* Viewer.

Supplemental table

Table S1. Primer sequences used in this study

Gene	Species	Forward primer	Reverse primer
18S	Mouse	TTCTGGCCAACGGTCTAGACAAC	CCAGTGGTCTTGGTGTGCTGA
Ucp1	Mouse	CACCTTCCCGCTGGACACT	CCCTAGGACACCTTTATACCTAATGG
Pgc1	Mouse	AGCCGTGACCACTGACAACGAG	GCTGCATGGTTCTGAGTGCTAAG
Cidea	Mouse	ATCACAACTGGCCTGGTTACG	TACTACCCGGTGTCCATTTCT
Cox8	Mouse	GAACCATGAAGCCAACGACT	GCGAAGTTCACAGTGGTTCC
aP2	Mouse	ACACCGAGATTTCCTTCAAACTG	CCATCTAGGGTTATGATGCTCTTCA
Zip13	Mouse	AGGCCCCCAGCAAAGACCCCA	CTTTTTGCTCACAAGGAAGCT
Cpt1b	Mouse	GTCGCTTCTTCAAGGTCTGG	AAGAAAGCAGCACGTTCGAT
Cpt2	Mouse	CAGCACAGCATCGTACCCA	TCCCAATGCCGTTCTCAAAAT
Fasn	Mouse	GAGGTGGTGATAGCCGGTAT	TGGGTAATCCATAGAGCCCAG
CD36	Mouse	TGCATTTGCCAATGTCTAGC	CCCTCCAGAATCCAGACAAC
ACC	Mouse	AATGAACGTGCAATCCCATTTG	ACTCCACATTTGCGTAATTGTTG
Scd1	Mouse	AGGCCTGTACGGGATCATACT	AGAGCGCTGGTCATGTAGTAG
ATGL	Mouse	TTCGCAATCTCTACCGCCTC	TGGTTCAGTAGGCCATTCCTC
Elovl3	Mouse	TCCGCGTTCTCATGTAGGTCT	GGACCTGATGCAACCCTATGA
HSL	Mouse	GCGCTGGAGGAGTGTTTTT	CCGCTCTCCAGTTGAACC
MGL	Mouse	AGGCGAACTCCACAGAATGTT	ACAAAAGAGGTACTGTCCGTCT
Plin1	Mouse	CTGTGTGCAATGCCTATGAGA	CTGGAGGGTATTGAAGAGCCG
PPARg	Mouse	GTGCCAGTTTCGATCCGTAG	GGCCAGCATCGTGTAGATGA
Pde3b	Mouse	CCAATTCCTGGCTTACCTCA	GCAATCTGTCCAGAACCAAG
MT1	Human	AGAGTGCAAATGCACCTCCTGC	CGGACATCAGGCACAGCAGCT
GAPDH	Human	CGAGATCCCTCCAAAATCAA	CATGAGTCCTTCCACGATACCAA

Supplemental methods

Measurement of food intake of mice

Food intake of mice was measured every day for 5 days. The average food intake of 1 day is shown. During the measurement period, mice were housed in individual cages.

Measurement of rectal temperature of mice

Rectal temperatures of mice were measured using a D717 pocket-sized thermistor (Takara Thermistor, Yokohama, Japan). For cold tolerance test, mice were placed around 7 a.m. in individual cages in 23℃ without diet, and after 5 hours mice were exposed at 4℃ without diet and measured the rectal temperature.

Measurement of blood glucose levels and insulin levels of mice

The IPGTT and insulin tolerance test (ITT) were performed as described previously (1, 2) . For IPGTT, animals were fasted for 13 h, and then injected i.p. with 2 g/kg glucose. Glucose levels were measured using a glucose analyzer (Glutest Mint, Sanwa Chemical Co., Japan). Insulin levels were measured using an ELISA kit (Morinaga Co., Kanagawa, Japan). For the ITT, mice were injected i.p. with insulin (0.75 units/kg).

Body composition analysis using micro-CT

CT was performed on mice under isoflurane anesthesia using a LaTheta micro-CT scanner

(Hitachi, Tokyo, Japan). The abdominal region between the first and sixth lumbar vertebrae was scanned, and the sizes of the fat and soft tissue compartments were measured.

Tissue histology

For H&E staining, the tissues of mice were fixed in 4% paraformaldehyde overnight at 4 °C, followed by dehydration in 70% ethanol. After the dehydration procedure, tissues were embedded in paraffin, sectioned at a thickness of 5 μm, and stained with H&E following a standard protocol.

Measurement of hydroxyl radical levels

Hydroxyl radical levels were measured using hydroxyphenyl fluorescein (HPF) (Goryo Chemical, #SK3001-01). Cells were plated onto 24-well plates, and washed with Hanks' Balanced Salt Solution (HBSS) buffer (Sigma-Aldrich) 3 times. The cells were then incubated with 10 μM HPF for 30 min, add then DMSO or isoproterenol was added and cells were incubated for a further 30 min, and washed with HBSS buffer 3 times. Fluorescence was recorded at 490 nm excitation and 515 nm emission using EnSpire multimode plate reader (Perkin Elmer). For protein concentration determination, cells were lysed with 250 μL lysis solution (0.3 N NaOH/0.1% SDS), and incubated at room temperature under vigorous shaking. Protein content was determined using Pierce 660 nm protein assay reagent, using BSA as a

187 standard.

188

189 **Detection of HA signals in live *X. laevis* oocytes**

190 Live *X. laevis* oocytes expressing 4F2hc-m13-HA were treated with an anti-HA antibody before
191 fixing and sectioning to confirm the topology of the fusion protein. Two days after the injection
192 of the cRNA, *X. laevis* oocytes were cooled and blocked with cold ND96 buffer containing
193 16% goat serum (NDGS) for 30 min at 4 °C, and treated with an anti-HA antibody (1:100;
194 BioLegend, San Diego, USA, #90154) diluted with NDGS for 1 h at 4 °C. After three cycles
195 of 5 min washes with ice-cold NDGS, oocytes were rinsed with ND96 and fixed with 4%
196 paraformaldehyde for 30 min followed by embedding in OCT compound. Ten μm-thick frozen
197 sliced sections were blocked with 10% goat serum and 1% Triton X-100 in PBS for 30 min,
198 and incubated with Alex488-conjugated anti-mouse IgG antibody (1:100; Thermo Fisher
199 Scientific, Waltham, MA, USA) for 1 h at RT. After three 5 min washes with PBS-T, the
200 sections were mounted in fluorescence mounting medium (Fluoro-KEEPER, Nacalai Tesque,
201 Kyoto, Japan), and observed using a confocal microscope (FV1000).

202

203 **Determination of kinetics parameters**

204 To determine the kinetics parameters of Zn^{2+} and Fe^{2+} uptake in 4Fhc-m13 expressing oocytes,
205 the uptake assays were performed at 7 different concentrations (15 - 200 μM) of the metals for
206 120 min. Initial uptake rates were estimated from the values for 120 min, which is in the linear

range of the time course experiments. The uptake rates for 4F2hc-m13 were calculated by subtracting those of the control oocytes, and plotted against metal concentration. The kinetics parameters (V_{max}, Km) were determined by non-linear curve fitting to the Michaelis-Menten equation using R software (version 4.3.1) with the drc package (version 3.0-1).

Measurement of Fe^{2+} levels within mitochondria

Labile iron levels within mitochondria were measured using Mito-FerroGreen (M489, DOJINDO, Kumamoto, Japan) and MitoTracker (M7512, Invitrogen) to confirm that all Mito-FerroGreen signals were merged with the MitoTracker signals. Signals were observed using a confocal microscope (FV1000), and images were quantified by ImageJ software.

***Pde3b* knockdown**

Pde3b knockdown was performed in adipocytes according to a previously described protocol (3). Briefly, siRNA specific to the *Pde3b* gene (L-043781-00) and control nontargeting siRNA (D-001810-10) were purchased from Dharmacon. siRNA was transfected using RNAiMax (Invitrogen), and incubated for 6 h. The medium was exchanged with fresh differentiation medium, and incubated for an additional 66 h. Specific knockdown of *Pde3b* was confirmed using qRT-PCR.

ICP-MS

For the determination of Fe and Zn levels in mature adipocytes, mature adipocytes from subcutaneous and visceral adipose tissues were harvested as described in the main Methods. ICP-MS analysis was conducted as described in the main Methods, except that 1 mL of HNO_3 was used and the final volume was set to 10 mL. Furthermore, the blank sample was prepared using 0.1 mL of KRB buffer and analyzed in the same manner. The amounts of Fe and Zn were corrected by subtracting the amounts of these elements present in the residual buffer.

References

1 Tamaki, M. *et al.* The diabetes-susceptible gene SLC30A8/ZnT8 regulates hepatic insulin clearance. *J Clin Invest* **123**, 4513-4524 (2013). https://doi.org/10.1172/JCI68807

2 Shigihara, N. *et al.* Human IAPP-induced pancreatic beta cell toxicity and its regulation by autophagy. *J Clin Invest* **124**, 3634-3644 (2014). https://doi.org/10.1172/JCI69866

3 Strnadova, M., Thor, D. & Kaczmarek, I. Protocol for changing gene expression in 3T3-L1 (pre)adipocytes using siRNA-mediated knockdown. *STAR Protoc* **5**, 103075 (2024). https://doi.org/10.1016/j.xpro.2024.103075

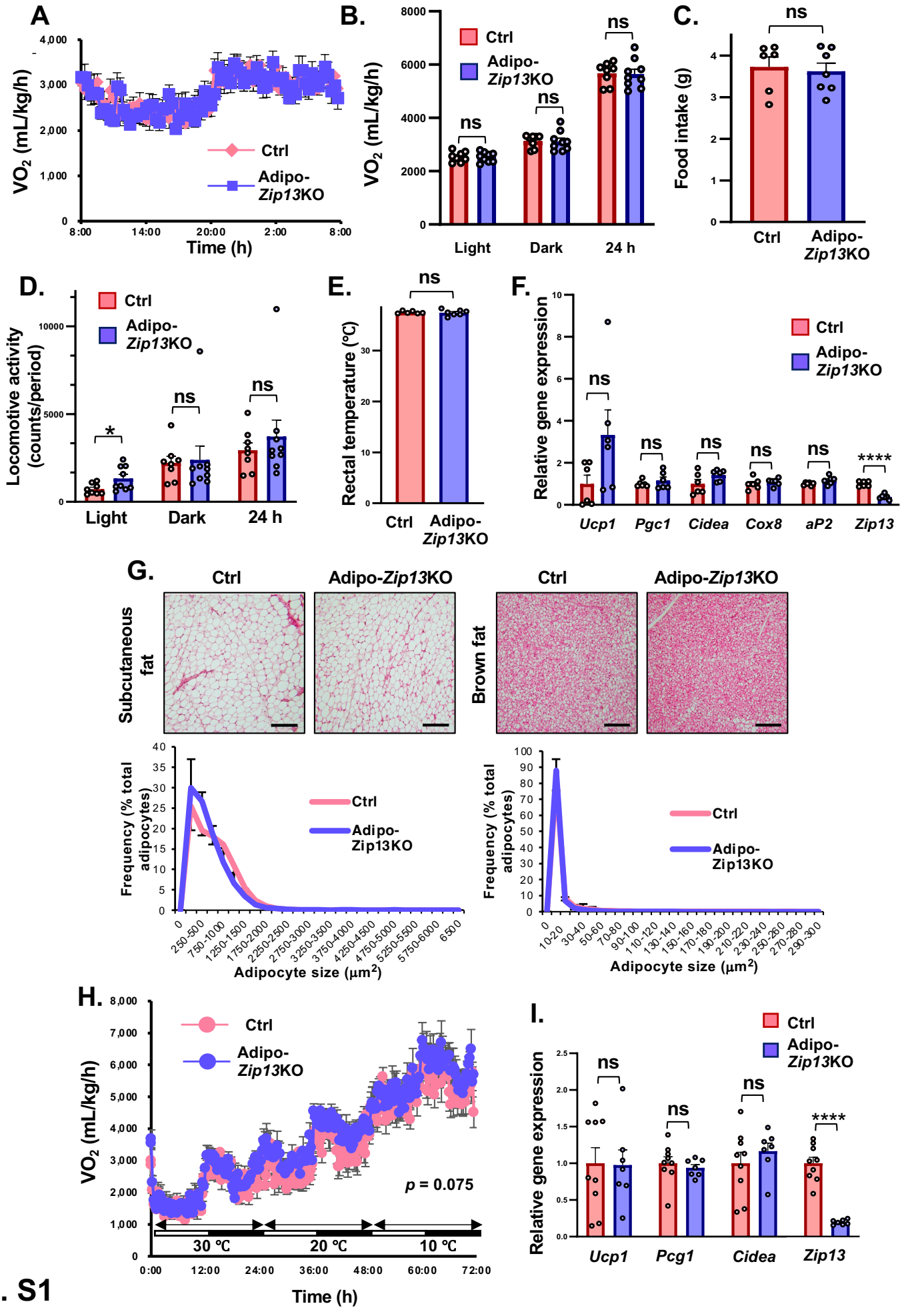
A
VO2 (mL/kg/h)
Time (h)
Ctrl
Adipo-Zip13KO
B.
VO2 (mL/kg/h)
Light
Dark
24 h
ns
C.
Food intake (g)
D.
Locomotive activity (counts/period)
*
E.
Rectal temperature (℃)
F.
Relative gene expression
Ucp1
Pgc1
Cidea
Cox8
aP2
Zip13
****
G.
Subcutaneous fat
Brown fat
Frequency (% total adipocytes)
Adipocyte size (μm2)
H.
p = 0.075
30 ℃
20 ℃
10 ℃
I.

Fig. S1

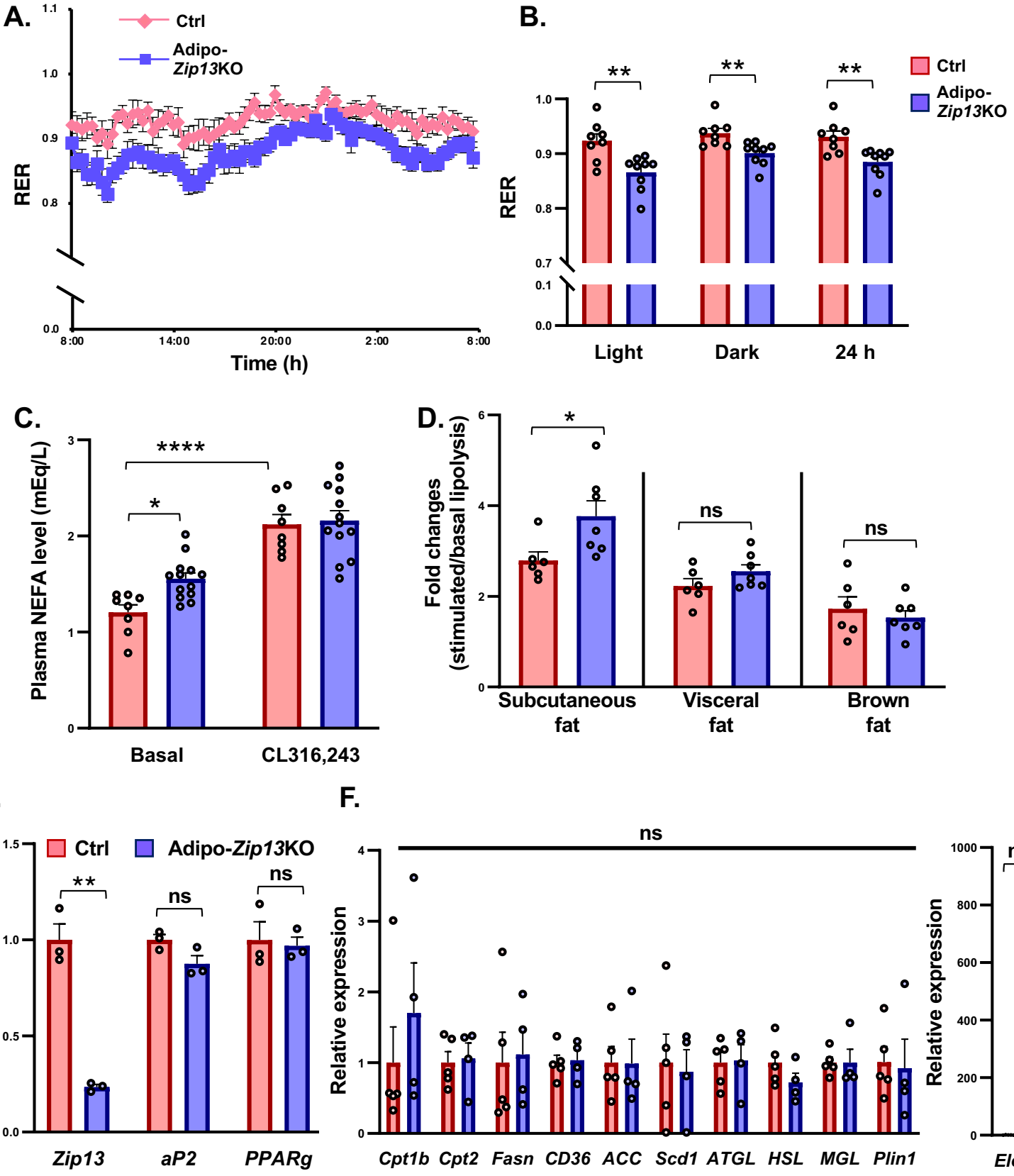
A.
Ctrl
Adipo-Zip13KO
RER
Time (h)
B.
Ctrl
Adipo-Zip13KO
RER
Light
Dark
24 h
C.
Plasma NEFA level (mEq/L)
Basal
CL316,243
D.
Fold changes (stimulated/basal lipolysis)
Subcutaneous fat
Visceral fat
Brown fat
E.
Ctrl
Adipo-Zip13KO
Relative expression
Zip13
aP2
PPARg
F.
Relative expression
Cpt1b
Cpt2
Fasn
CD36
ACC
Scd1
ATGL
HSL
MGL
Plin1
Elovl3

Fig. S2

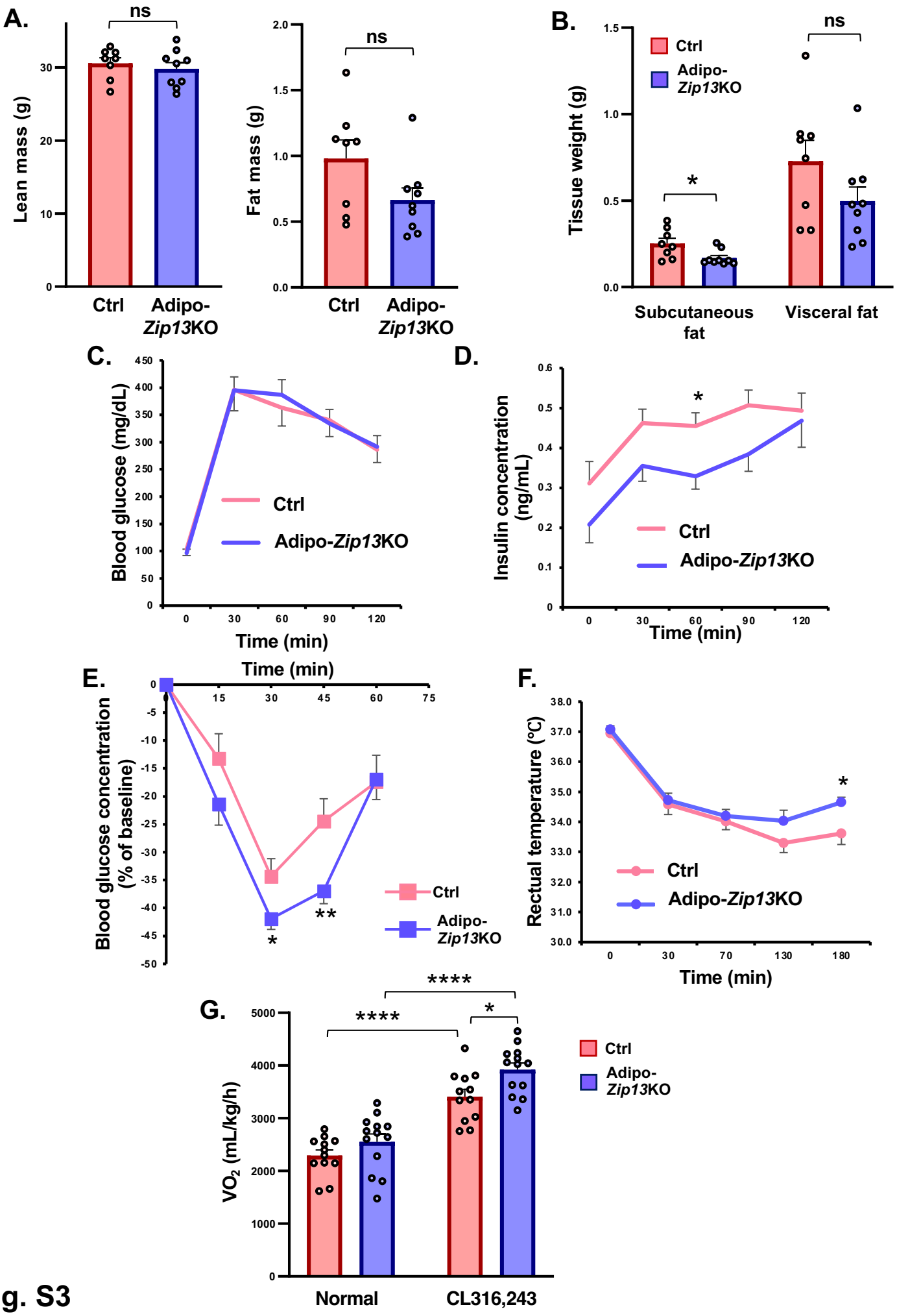
A.
ns
Lean mass (g)
Ctrl
Adipo-Zip13KO
ns
Fat mass (g)
Ctrl
Adipo-Zip13KO
B.
Ctrl
Adipo-Zip13KO
Tissue weight (g)
*
ns
Subcutaneous fat
Visceral fat
C.
Blood glucose (mg/dL)
Ctrl
Adipo-Zip13KO
Time (min)
D.
Insulin concentration (ng/mL)
*
Ctrl
Adipo-Zip13KO
Time (min)
E.
Time (min)
Blood glucose concentration (% of baseline)
*
**
Ctrl
Adipo-Zip13KO
F.
Rectual temperature (°C)
*
Ctrl
Adipo-Zip13KO
Time (min)
G.
****
****
*
VO2 (mL/kg/h)
Ctrl
Adipo-Zip13KO
Normal
CL316,243

Fig. S3

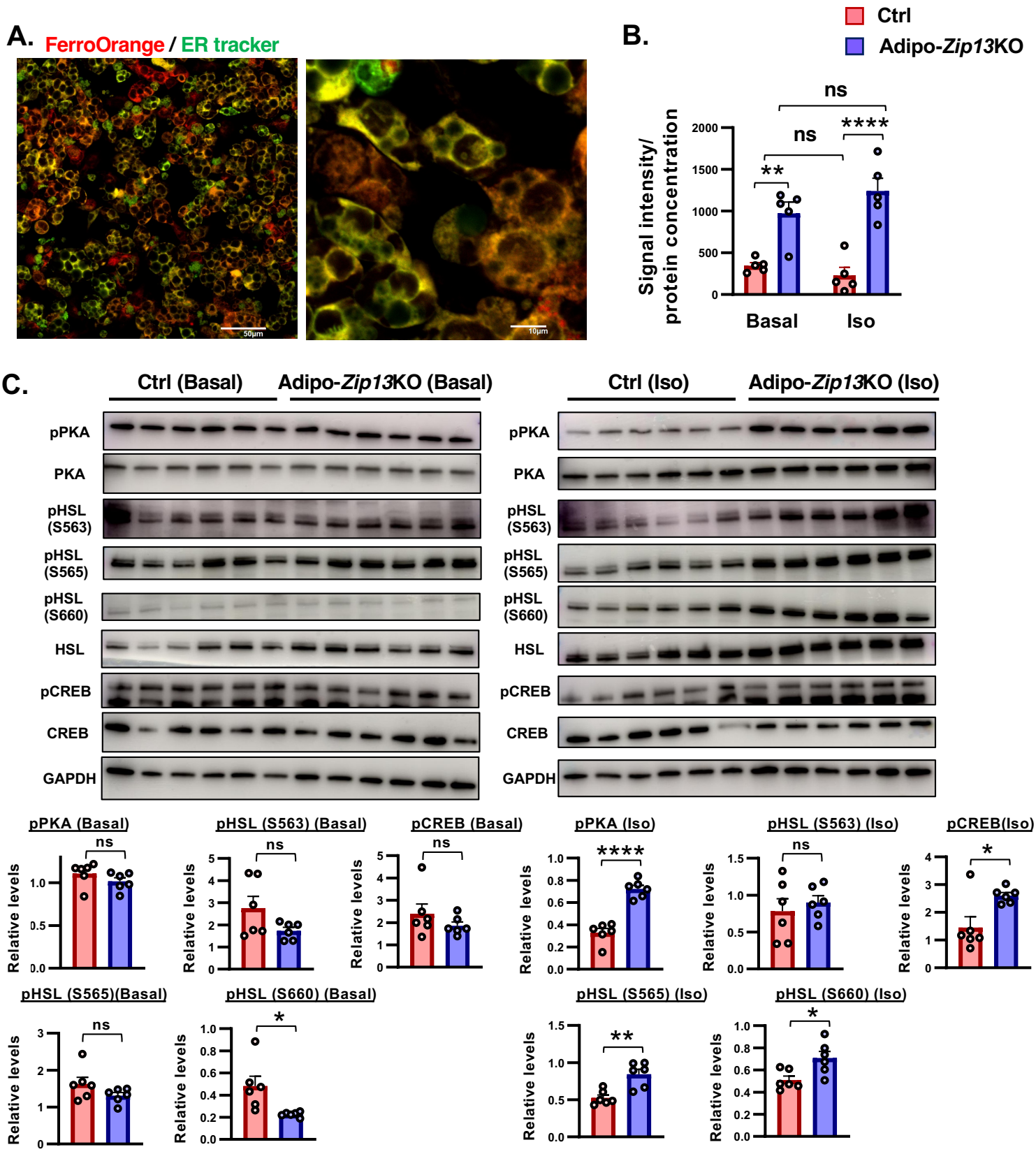
A.
FerroOrange / ER tracker
50μm
10μm
B.
Ctrl
Adipo-Zip13KO
Signal intensity/ protein concentration
2000
1500
1000
500
0
ns
ns
****
**
Basal
Iso
C.
Ctrl (Basal)
Adipo-Zip13KO (Basal)
Ctrl (Iso)
Adipo-Zip13KO (Iso)
pPKA
PKA
pHSL (S563)
pHSL (S565)
pHSL (S660)
HSL
pCREB
CREB
GAPDH
pPKA (Basal)
pHSL (S563) (Basal)
pCREB (Basal)
pPKA (Iso)
pHSL (S563) (Iso)
pCREB(Iso)
pHSL (S565)(Basal)
pHSL (S660) (Basal)
pHSL (S565) (Iso)
pHSL (S660) (Iso)
Relative levels
ns
****
*
**

Fig. S4

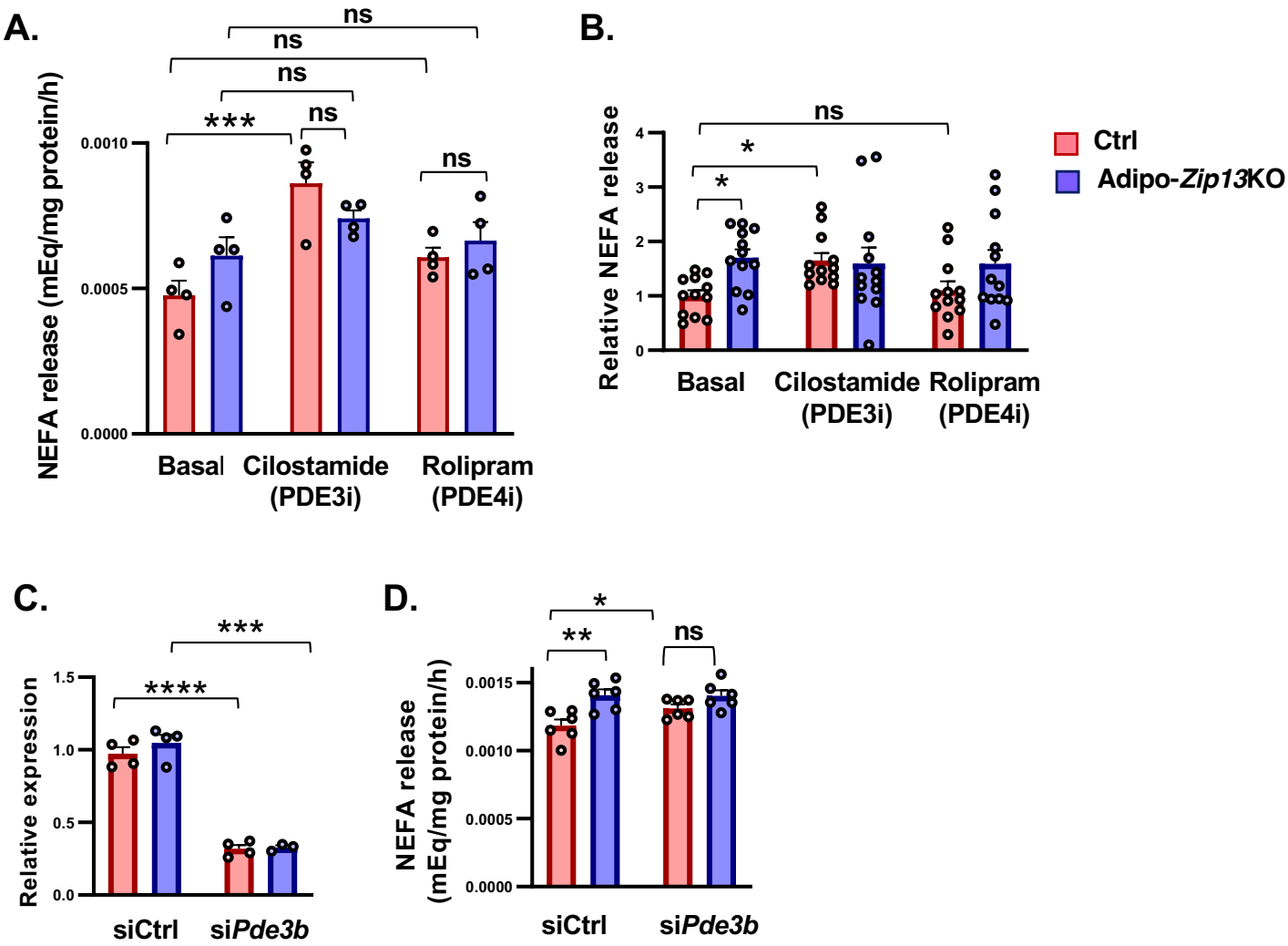
A.
B.
C.
D.
NEFA release (mEq/mg protein/h)
Relative NEFA release
Relative expression
Basal
Cilostamide (PDE3i)
Rolipram (PDE4i)
Ctrl
Adipo-Zip13KO
siCtrl
siPde3b
ns
***
****
**
*

Fig. S5

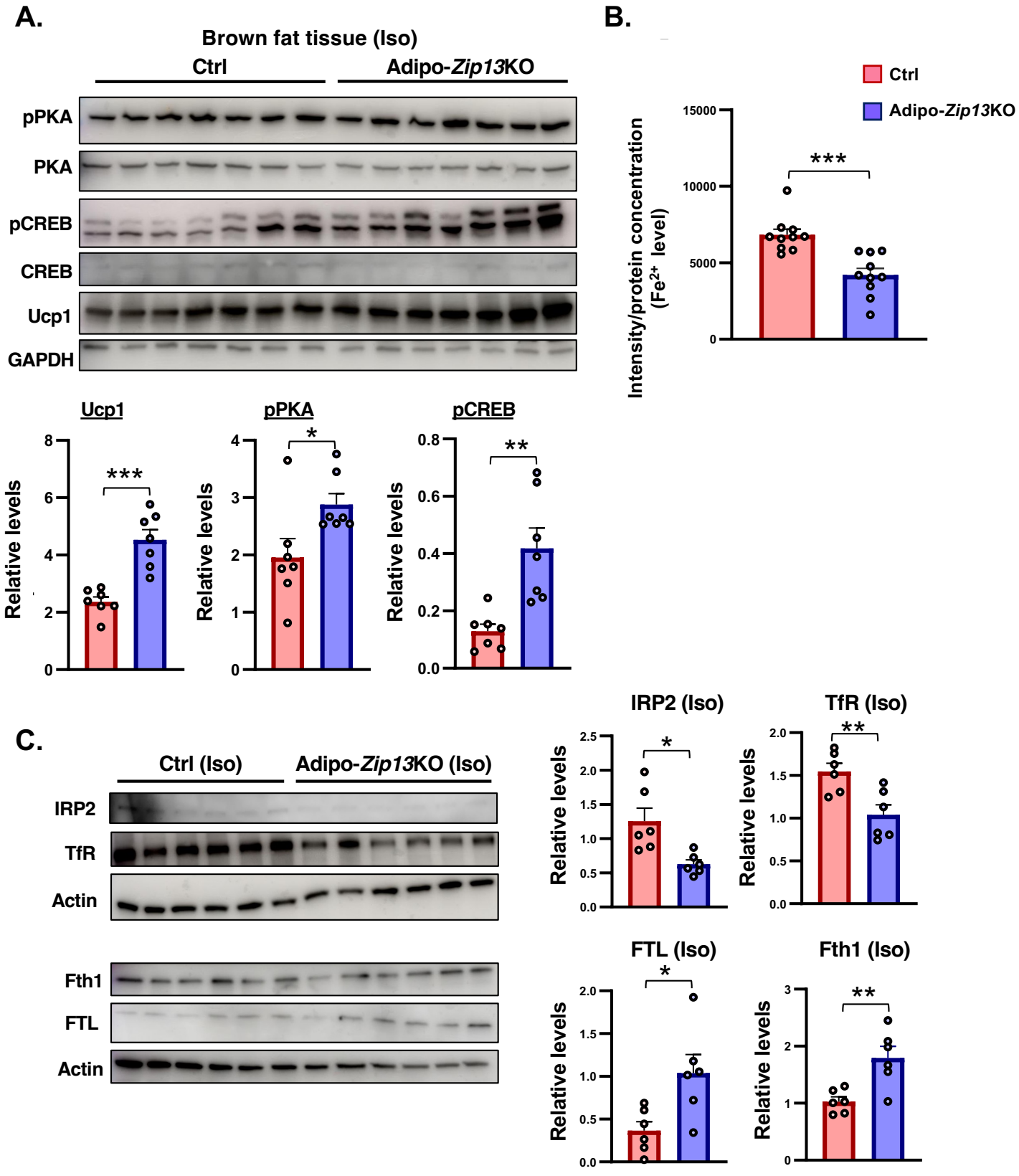
A.
Brown fat tissue (Iso)
Ctrl
Adipo-Zip13KO
pPKA
PKA
pCREB
CREB
Ucp1
GAPDH
Ucp1
pPKA
pCREB
Relative levels
***
*
**
B.
Ctrl
Adipo-Zip13KO
Intensity/protein concentration (Fe2+ level)
***
C.
Ctrl (Iso)
Adipo-Zip13KO (Iso)
IRP2
TfR
Actin
Fth1
FTL
Actin
IRP2 (Iso)
TfR (Iso)
FTL (Iso)
Fth1 (Iso)
Relative levels

Fig. S6

Injection: **mZIP13-HA**

HA **DIC**

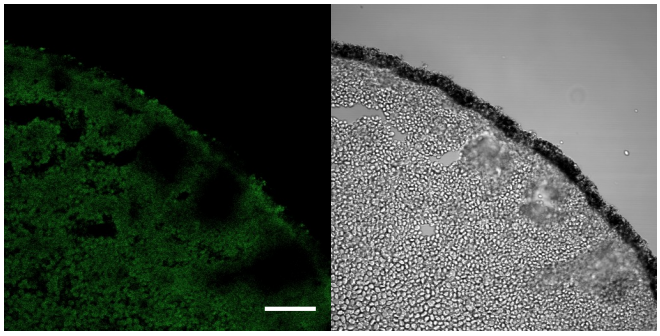

Injection: **4F2hc-m13-HA**

HA **DIC**

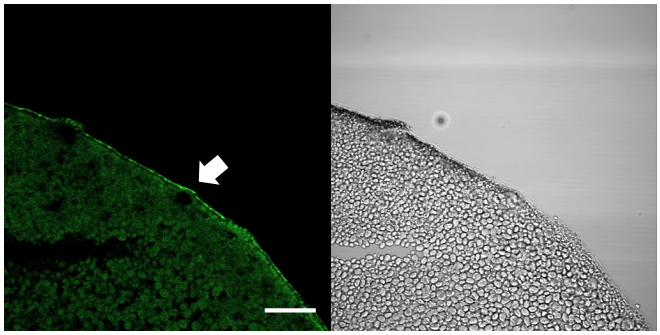

Fig. S7

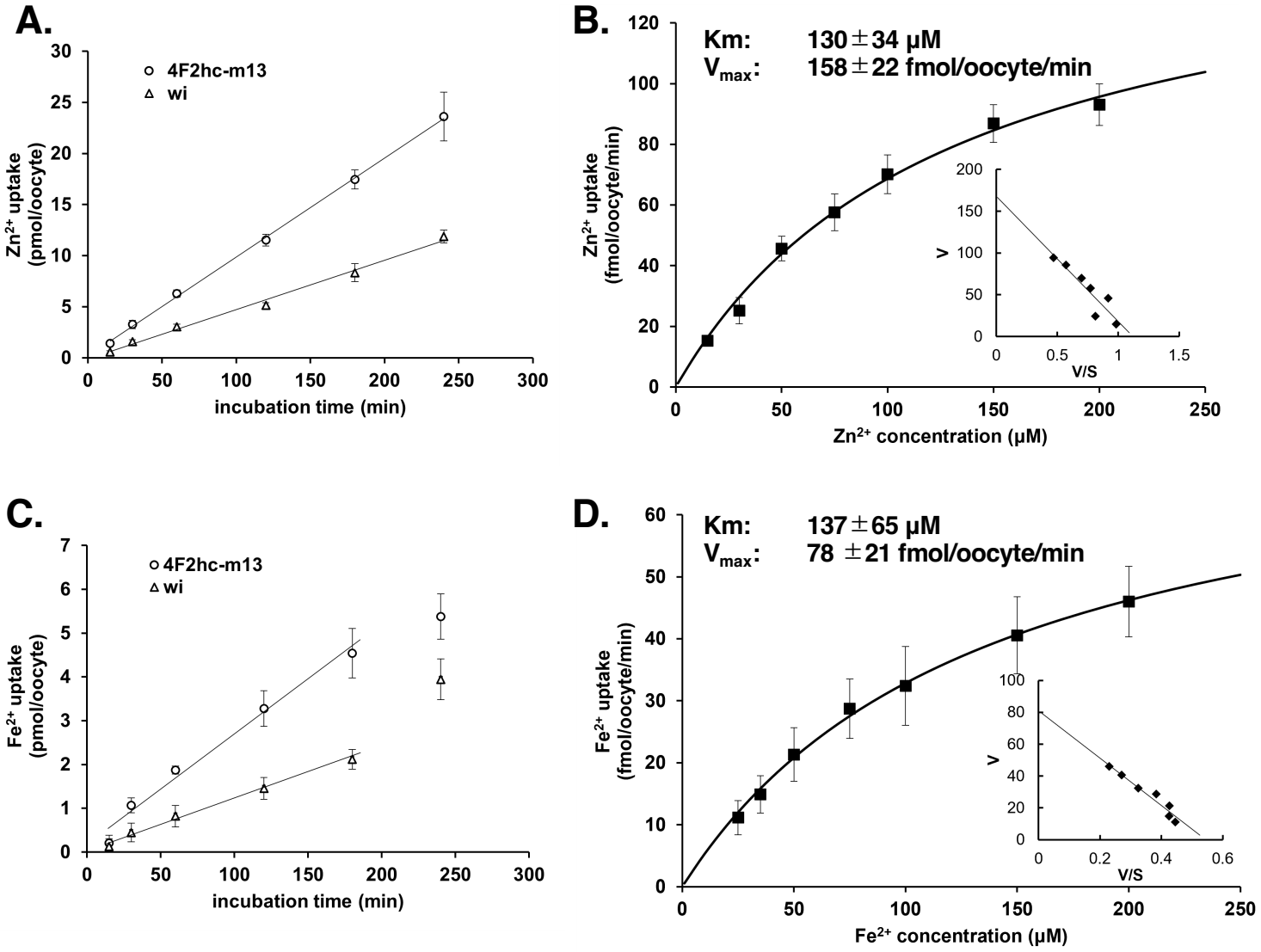
A.
4F2hc-m13
wi
Zn2+ uptake (pmol/oocyte)
incubation time (min)
B.
Km: 130±34 μM
Vmax: 158±22 fmol/oocyte/min
Zn2+ uptake (fmol/oocyte/min)
Zn2+ concentration (μM)
V
V/S
C.
4F2hc-m13
wi
Fe2+ uptake (pmol/oocyte)
incubation time (min)
D.
Km: 137±65 μM
Vmax: 78 ±21 fmol/oocyte/min
Fe2+ uptake (fmol/oocyte/min)
Fe2+ concentration (μM)
V
V/S

Fig. S8

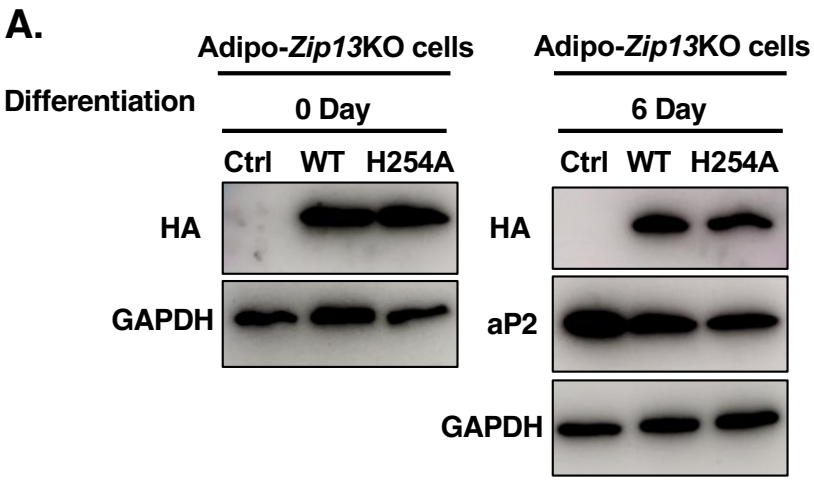
A.
Adipo-Zip13KO cells
Adipo-Zip13KO cells
Differentiation
0 Day
6 Day
Ctrl WT H254A
Ctrl WT H254A
HA
GAPDH
HA
aP2
GAPDH

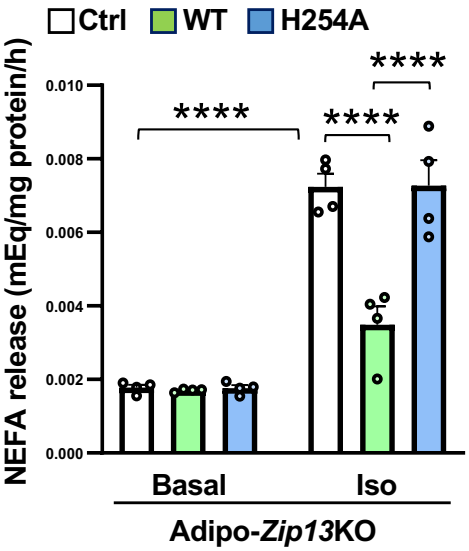
B.
Ctrl
WT
H254A
NEFA release (mEq/mg protein/h)
0.010
0.008
0.006
0.004
0.002
0.000
****
****
****
Basal
Iso
Adipo-Zip13KO

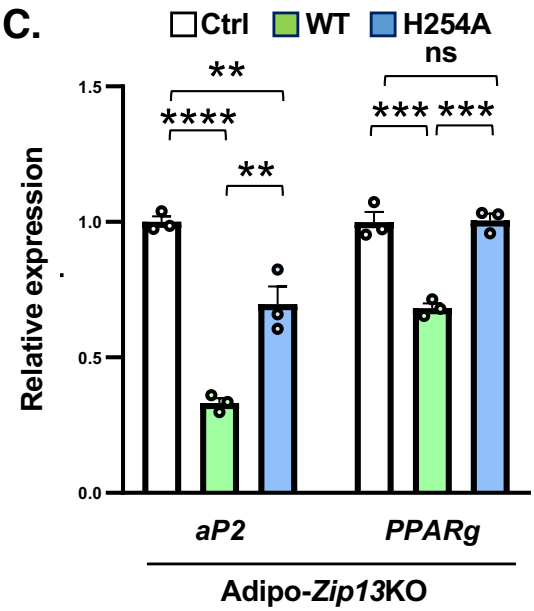
C.
Ctrl
WT
H254A
Relative expression
1.5
1.0
0.5
0.0
**
****
**
ns
*** ***
aP2
PPARg
Adipo-Zip13KO

Fig. S9

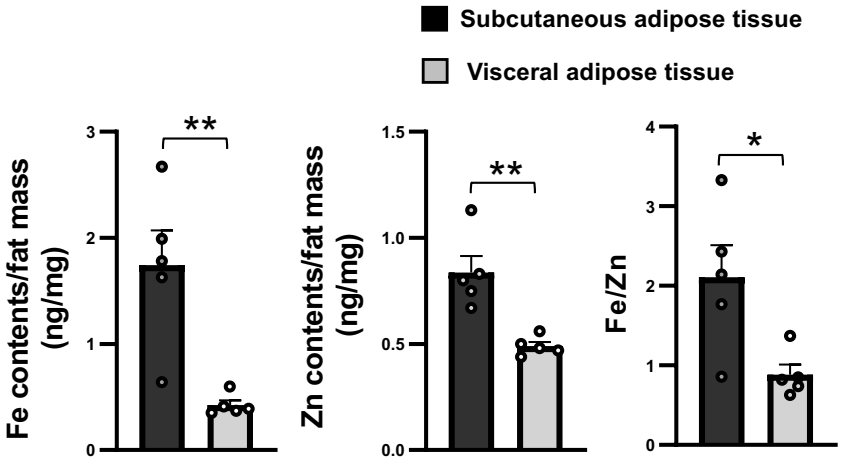
Subcutaneous adipose tissue
Visceral adipose tissue
Fe contents/fat mass (ng/mg)
Zn contents/fat mass (ng/mg)
Fe/Zn
**
**
*
0
1
2
3
0.0
0.5
1.0
1.5
4

Fig. S10

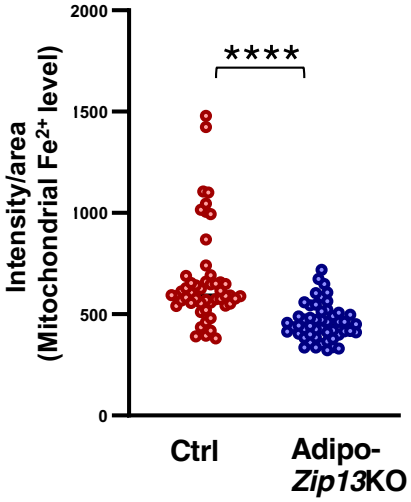
2000
1500
1000
500
0
****
Intensity/area
(Mitochondrial Fe2+ level)
Ctrl
Adipo-
Zip13KO

Fig. S11

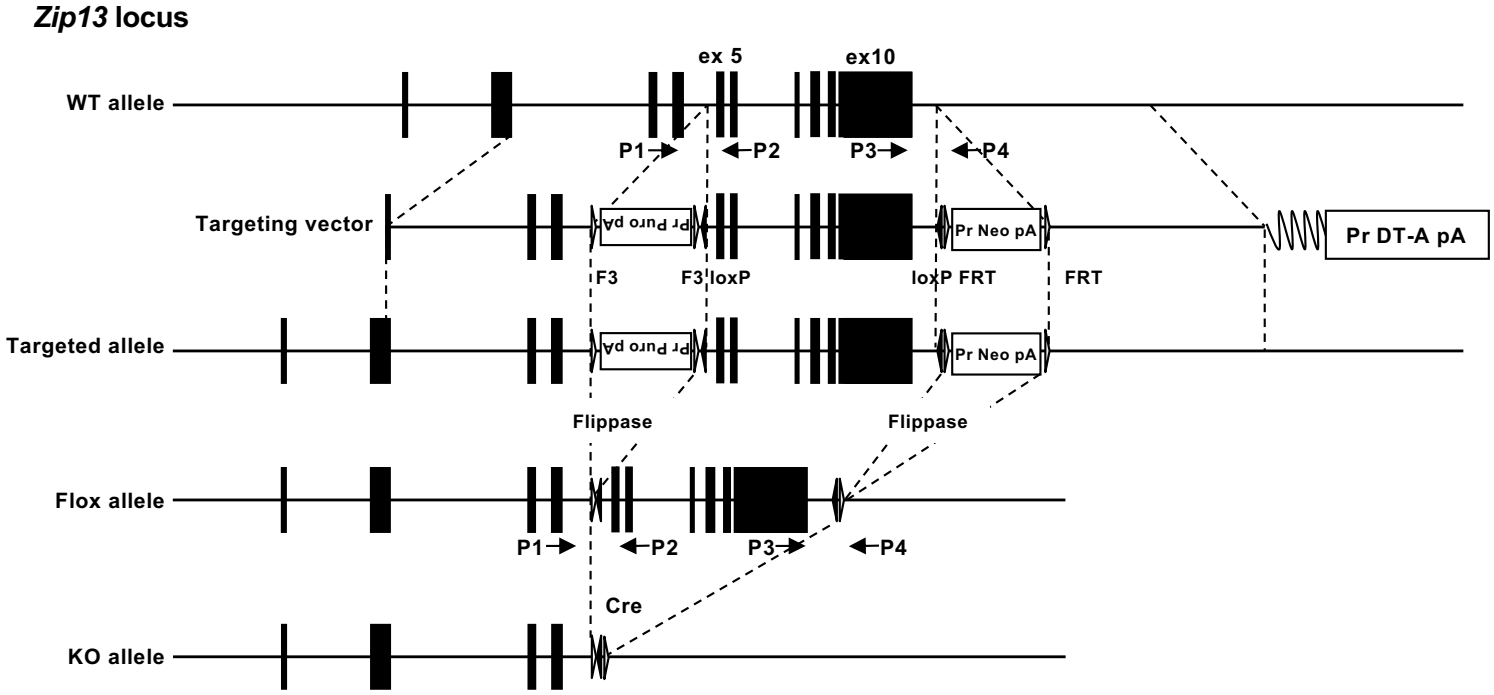
Zip13 locus
ex 5
ex10
WT allele
P1
P2
P3
P4
Targeting vector
Pr Puro pA
Pr Neo pA
Pr DT-A pA
F3
F3
loxP
loxP
FRT
FRT
Targeted allele
Pr Puro pA
Pr Neo pA
Flippase
Flippase
Flox allele
P1
P2
P3
P4
Cre
KO allele

Fig. S12

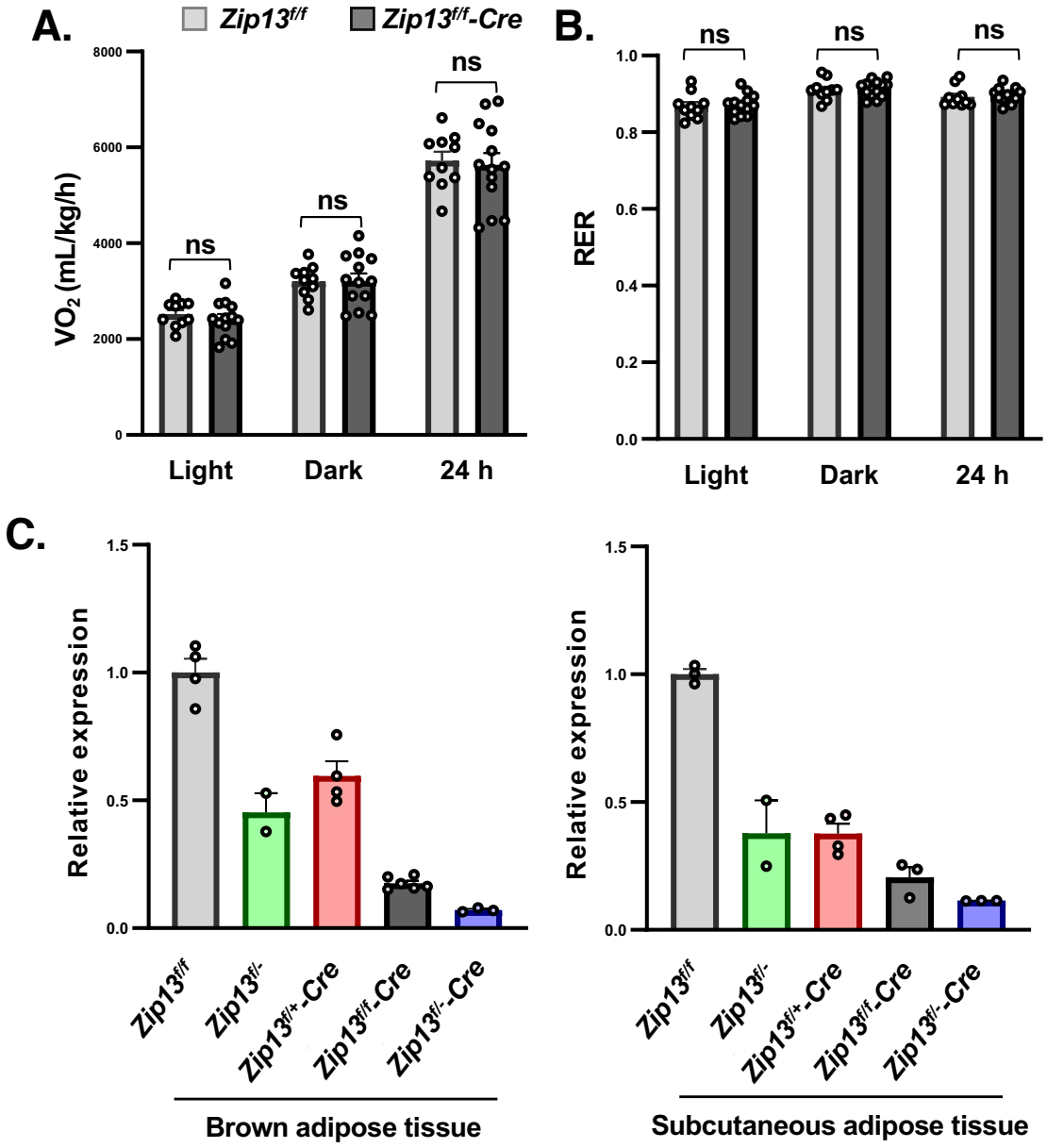
A.
Zip13f/f
Zip13f/f-Cre
VO2 (mL/kg/h)
8000
6000
4000
2000
0
ns
ns
ns
Light
Dark
24 h
B.
RER
1.0
0.8
0.6
0.4
0.2
0.0
ns
ns
ns
Light
Dark
24 h
C.
Relative expression
1.5
1.0
0.5
0.0
Zip13f/f
Zip13f/-
Zip13f/+-Cre
Zip13f/f-Cre
Zip13f/--Cre
Brown adipose tissue
Relative expression
1.5
1.0
0.5
0.0
Zip13f/f
Zip13f/-
Zip13f/+-Cre
Zip13f/f-Cre
Zip13f/--Cre
Subcutaneous adipose tissue

Fig. S13

4F2hc-m13 (rank 1)
mZIP13(Q8BZH0)
RMSD: 0.37Å

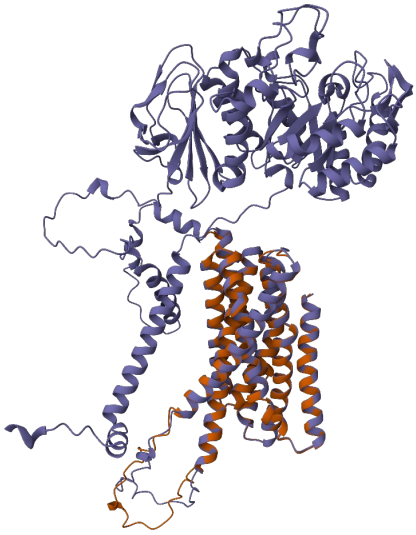

4F2hc-m13 (rank 2)
mZIP13(Q8BZH0)
RMSD: 0.47Å

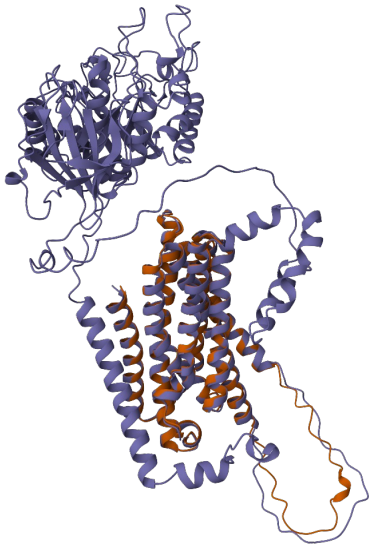

4F2hc-m13 (rank 3)
mZIP13(Q8BZH0)
RMSD: 0.47Å

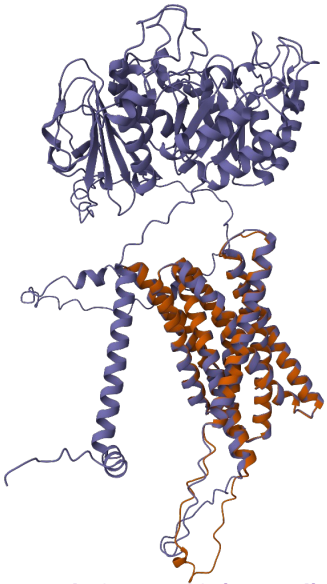

4F2hc-m13 (rank 4)
mZIP13 Q8BZH0)
RMSD: 0.47Å

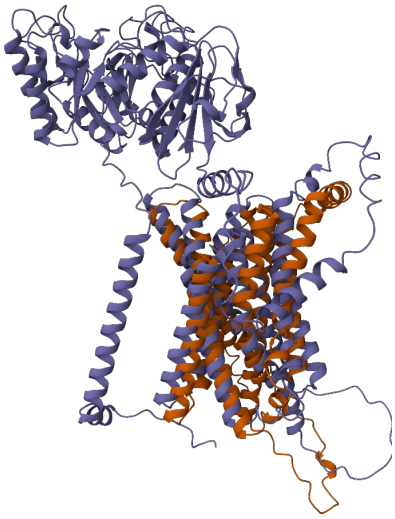

4F2hc-m13 (rank 5)
mZIP13(Q8BZH0)
RMSD: 5.36Å

Fig. S14

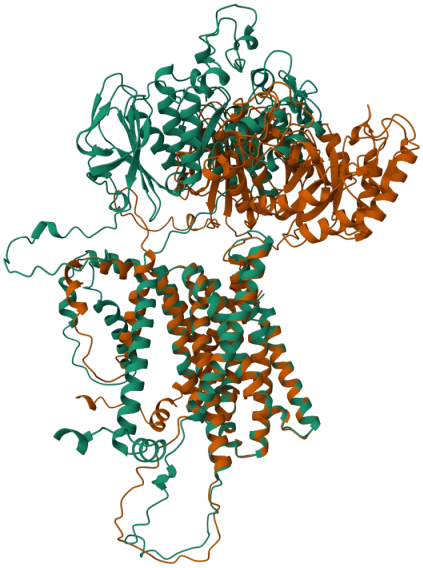

4F2hc-m13 (rank 1)
4F2hc-m13 (rank 2)
RMSD: 0.52Å

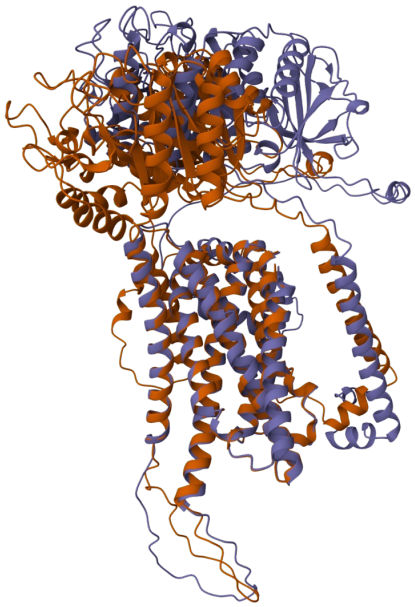

4F2hc-m13 (rank 1)
4F2hc-m13 (rank 3)
RMSD: 0.44 Å

4F2hc-m13 (rank 1)
4F2hc-m13 (rank 4)
RMSD: 0.54Å

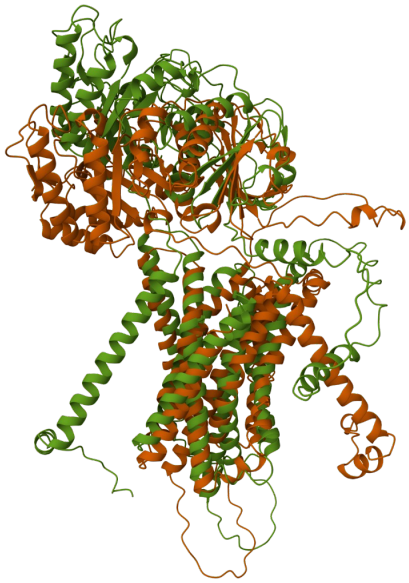

4F2hc-m13 (rank 1)
4F2hc-m13 (rank 5)
RMSD: 5.36Å

Fig. S15